Human Eye Development Is Characterized by Coordinated Expression of Fibrillin Isoforms

Dirk Hubmacher,[1] Dieter P. Reinhardt,[2] Thomas Plesec,[3] Katja Schenke-Layland,[4–6] and Suneel S. Apte[1]

[1]Department of Biomedical Engineering, Cleveland Clinic, Lerner Research Institute, Cleveland, Ohio, United States
[2]Faculty of Medicine and Faculty of Dentistry, McGill University, Montreal, Quebec, Canada
[3]Cleveland Clinic, Department of Anatomic Pathology, Cleveland, Ohio, United States
[4]Department of Women's Health, University Women's Hospital, Eberhard-Karls-University, Tübingen, Germany
[5]Department of Cell and Tissue Engineering, Fraunhofer IGB Stuttgart, Stuttgart, Germany
[6]Department of Medicine/Cardiology, Cardiovascular Research Laboratories, David Geffen School of Medicine at University of California Los Angeles, Los Angeles, California, United States

Correspondence: Dirk Hubmacher, Department of Biomedical Engineering, Lerner Research Institute, Cleveland Clinic, 9500 Euclid Avenue, Cleveland, OH 44195, USA; hubmacd@ccf.org.
Suneel S. Apte, Department of Biomedical Engineering, Lerner Research Institute, Cleveland Clinic, 9500 Euclid Avenue, Cleveland, OH 44195, USA; aptes@ccf.org.

Submitted: August 12, 2014
Accepted: October 25, 2014

Citation: Hubmacher D, Reinhardt DP, Plesec T, Schenke-Layland K, Apte SS. Human eye development is characterized by coordinated expression of fibrillin isoforms. *Invest Ophthalmol Vis Sci*. 2014;55:7934–7944. DOI: 10.1167/iovs.14-15453

Purpose. Mutations in human fibrillin-1 and -2, which are major constituents of tissue microfibrils, can affect multiple ocular components, including the ciliary zonule, lens, drainage apparatus, cornea, and retina. However, the expression pattern of the three human fibrillins and an integral microfibrillar component, MAGP1, during human eye development is not known.

Methods. We analyzed sections from human eyes at gestational weeks (GWs) 6, 8, and 11 and at 1 and 3 years of age with antibodies specific for each human fibrillin isoform or MAGP1, using immunofluorescence microscopy.

Results. During embryonic development, each fibrillin isoform was detected in vascular structures bridging the ciliary body and the developing lens, hyaloid vasculature, and retina. In addition, they were present in the developing corneal basement membranes and lens capsule. MAGP1 codistributed with the fibrillin isoforms. In contrast, the juvenile zonule was composed of fibrillin-1 microfibrils containing MAGP1, but fibrillin-2 was absent and fibrillin-3 was only sparsely detected.

Conclusions. Fibrillin-1, -2, and, unique to humans, fibrillin-3 are found in various ocular structures during human embryonic eye development, whereas fibrillin-1 dominates the postnatal zonule. We speculate that vasculature spanning the ciliary body and lens, which elaborates fibrillin-2 and -3, may provide an initial scaffold for fibrillin assembly and zonule formation.

Keywords: fibrillin, extracellular matrix, ocular development, Marfan syndrome, ciliary zonule

Fibrillin microfibrils are found in association with elastic fibers and as isolated extracellular matrix (ECM) components in many tissues, such as the eye, the vasculature, the lung, and musculoskeletal system.[1] In the adult eye, fibrillin microfibrils comprise the ciliary zonule, a cell (and elastin)-free structure, which centers the lens in the optic path, and transmits ciliary muscle contraction and relaxation during accommodation.[2,3] The structure and function of fibrillin microfibrils is compromised in several human genetic disorders. Approximately 60% of affected individuals with Marfan syndrome (MFS; Online Mendelian Inheritance in Man [OMIM] #154700), which is caused by mutations in fibrillin-1 (*FBN1*) that are believed to result in haploinsufficiency, present with lens dislocation (ectopia lentis) and may develop glaucoma, corneal flattening, a higher incidence of retinal detachment than the general population, presenile cataract, and iris abnormalities.[4] Mutations in *FBN1* also cause dominantly inherited isolated ectopia lentis (OMIM #129600) and dominant Weill-Marchesani syndrome (WMS; OMIM #608328), in which ectopia lentis occurs in combination with microspherophakia, glaucoma, and short stature.[5–7] Mutations in fibrillin-2 (*FBN2*) cause Beals syndrome (congenital contractural arachnodactyly; OMIM #121050). Some reports of Beals syndrome have described severe myopia and compromised anterior segment structures, such as a defective ciliary zonule causing ectopia lentis, ciliary body hypoplasia, megalocornea, and iris and lens coloboma.[8] Mice deficient in *Fbn2* were recently found to have ocular developmental anomalies.[9] Thus, in addition to the well-established significance of FBN1 in the eye, FBN2 has an emerging role in development and developmental defects of the eye. Recently, polymorphisms in *FBN2* were associated with macular degeneration.[10] Fibrillin-3 has not been as extensively studied and no *FBN3* mutations affecting the eye are known.

In ectopia lentis observed in MFS, the fibers of the ciliary zonule appeared stretched or ruptured, consistent with a pathogenesis from haploinsufficiency, but in WMS, the problem appears to be aberrant formation of the zonule and the lens.[11,12] Therefore, insights on the composition and formation of the zonule are especially valuable in the context of microfibril disorders. FBN1, FBN2, and FBN3 can form homo- or heterotypic microfibrils.[13–15] Previous studies have indicated

that in general, FBN2 and FBN3 are predominantly expressed during embryogenesis, whereas FBN1 dominates in mature tissues.[16–18] In the adult human eye, fibrillin-1 was found in the zonule, ciliary body, the lens capsule and iris, and in both basement membranes of the cornea (i.e., the epithelial Bowman's membrane and endothelial Descemet membrane).[2] Mass spectrometry identified only fibrillin-1 and microfibril-associated glycoprotein 1 (MAGP1) in isolated human and bovine ciliary zonules.[19] Fibrillin-1 and -2 were previously localized in Bowman's membrane of the adult cornea.[20] In rodents, fibrillin-2, MAGP1, ADAMTS10, and latent-transforming growth factor-β binding protein 2 (LTBP2) are present in the ciliary zonule.[13,21,22] Interestingly, mutations in *ADAMTS10* or *LTBP2*, both found in association with microfibrils, and *ADAMTS17*, cause recessive WMS 1 (OMIM #277600), WMS 3/primary congenital glaucoma (OMIM #613086, #251750, #614819), and Weill-Marchesani-like syndrome (OMIM #613195), respectively.[23–26] In these eyes, ectopia lentis, microspherophakia, and, in the case of mutations in *LTBP2*, megalocornea, are present.[23,25,26] Mutations affecting an ADAMTS-like protein, ADAMTSL4, lead to recessive isolated ectopia lentis and ectopia lentis et pupillae (OMIM #225200, #225100).[27–29] Recent analysis of mouse ocular development identified strong developmental expression of *Fbn2* and showed that *Fbn1* knockout mice had a ciliary zonule composed of fibrillin-2 microfibrils.[13,21] Although the role of LTBP2 in the eye is not known, ablation of *Ltbp2* caused a loss of the ciliary zonules in mice.[13,22]

Collectively, therefore, these disorders of fibrillin and associated molecules (fibrillinopathies) would benefit from understanding their distribution in normal human eye development. The distribution of fibrillins in the human eye during the embryonic period and in children has not been previously determined. Together, the established (FBN1), emerging (FBN2), and potential (FBN3) significance for the fibrillins in eye disorders led to the present analysis of their distribution during human ocular development.

Methods

Tissue Specimens

Human embryonic eyes were obtained at gestational week (GW) 5 to 6 ($n = 3$), GW 8 ($n = 2$), and GW 11 ($n = 2$) from elective terminations of pregnancy and were fixed in 4% paraformaldehyde overnight (~14 hours) before paraffin embedding. One-year-old and 3-year-old human eyes ($n = 1$ for each age) were submitted for surgical pathology after enucleation from children for treatment of retinoblastoma and fixed in 10% formalin overnight before paraffin embedding. The use of sections from these specimens was without patient identifiers and was approved by the institutional review boards (IRBs) of the Cleveland Clinic, the University of California Los Angeles (UCLA), and the University Women's Hospital of the Eberhard-Karls-University Tübingen (UKT) (UCLA IRB #05-10-093; UKT IRB #356/2008BO2 and #406/2011BO1; to KSL). All procedures were performed in accordance with the tenets of the Declaration of Helsinki.

Immunofluorescence

All proteins were localized by an indirect immunofluorescence method in which the first antibody was specific to the antigen and the second antibody was fluorophore-conjugated. Sections of 5 to 6 μm, taken in the plane of the ocular axis, were deparaffinized and rehydrated to water. Antigen retrieval was performed by immersing the sections in 10 mM citric acid, 2 mM EDTA, 0.05% Tween-20, pH 6.2, and heating for 4 × 1.5 minutes at 50% power setting (450 Watt) with 30-second intermissions in a commercial microwave oven. Sections were washed briefly with distilled water, followed by 2 × 2-minute rinse in PBS containing 0.1% Tween-20, and a 5-minute rinse in PBS. Nonspecific binding was blocked using 5% normal goat serum (Jackson ImmunoResearch, West Grove, PA, USA) in PBS (blocking buffer) for 1 hour at room temperature. Sections were incubated overnight at 4°C with rabbit polyclonal antibodies raised against the C-terminal half of human fibrillin-1 and -3 (each diluted 1:750 in blocking buffer), the glycine-rich domain of fibrillin-2 (diluted 1:300), MAGP1 (diluted 1:300), collagen IV (Col IV; diluted 1:500; Rockland, Inc., Limerick, PA, USA), or rat monoclonal antibody against endomucin (1:100; eBioscience, San Diego, CA, USA). The generation and demonstration of the specificity of the fibrillin and MAGP1 antibodies has been described previously.[18,30,31] As a negative control, immunostaining was performed as above, using normal rabbit IgG (Santa Cruz Biotechnology, Dallas, TX, USA) at a concentration of 5 μg/mL as the first antibody. Sections were washed 3 × 10 minutes in PBS and incubated with fluorescent goat-anti-rat or goat-anti-rabbit secondary antibodies as appropriate (1:300 in blocking buffer, 1.5 hours at room temperature) (Jackson ImmunoResearch). Sections were washed 3 × 10 minutes in PBS and mounted with ProLong Gold anti-fade reagent containing 4′,6-diamidino-2-phenylindole (DAPI; Life Technologies, Carlsbad, CA, USA) to counterstain cell nuclei.

Microscopy

Sections were photographed using an upright fluorescent microscope equipped with a charge-coupled device camera (Microsystems, Buffalo Grove, IL, USA) at the Lerner Research Institute Imaging Core. Post acquisition image analysis was performed with ImageJ software (http://imagej.nih.gov/ij/; provided in the public domain by the National Institutes of Health, Bethesda, MD, USA).

Results

Specificity of the Fibrillin Antibodies

The monospecificity of polyclonal antibodies raised against human fibrillin-1, -2, and -3 was previously demonstrated using ELISA and staining of fibrillin-1 or fibrillin-2 knockout mouse embryonic fibroblasts and mouse eye sections.[13,18] Each antibody also gave distinct immunostaining in the present study, demonstrating the lack of cross-reactivity (e.g., Figs. 1B–D). The negative controls using normal rabbit IgG as first antibody resulted in no staining (see representative image in Supplementary Fig. S1).

Microfibril Staining of the Ciliary Zonule in the Infant and Juvenile Eye

In the 1- and 3-year-old human eyes, the ciliary zonule was evident by hematoxylin and eosin (H&E) staining (Fig. 1A) and stained strongly with the fibrillin-1 antibody, especially in the valleys between ciliary processes and at the zonule insertion in the lens girdle (Fig. 1B). There was no fibrillin-2 immunostaining of these zonules (Fig. 1C), but weak fibrillin-3 staining of zonule fibers adjacent to the unpigmented ciliary epithelium, its internal limiting membrane, and the lens capsule was observed (Fig. 1D). These results demonstrated that in the infant and juvenile eye, the ciliary zonule was predominantly

Investigative Ophthalmology & Visual Science

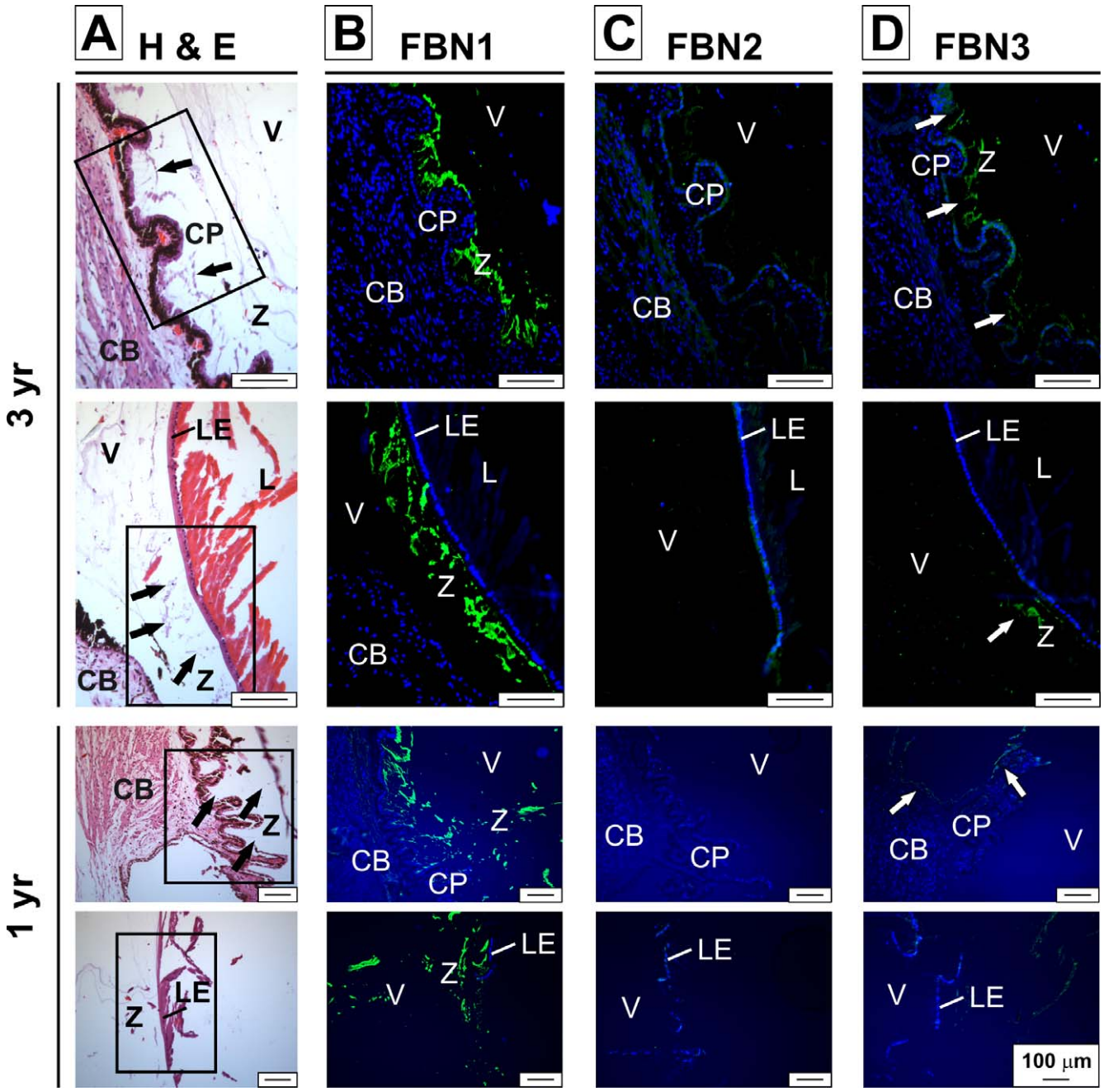

FIGURE 1. Distribution of fibrillin isoforms in the juvenile zonule. (**A**) Hematoxylin and eosin staining of a section from a 1-year-old and 3-year-old eye showing the zonule (*black arrows*) at its attachments to the ciliary body (*top*) and the lens (*bottom*). The boxed areas are depicted in (**B–D**). (**B–D**) Fibrillin immunostaining of the zonule showed strong fibrillin-1 (**B**) and some fibrillin-3 (**D**) staining marked with *white arrows*. Fibrillin-2 (**C**) was not detected. CB, ciliary body; CP, ciliary processes; L, lens; LE, lens epithelium; V, vitreous; Z, zonule. *Scale bars*: 100 μm.

composed of fibrillin-1 microfibrils, with fibrillin-3 present as an apparently minor constituent near each end of the zonule.

Fibrillins Are Found in the Vascular Structures Bridging the Developing Ciliary Body and the Lens

At GW 5 to 6 (Figs. 2A, 2B), the lens vesicle/developing lens was surrounded by an ECM containing fibrillin-1, -2, and -3. No fibrillin-containing fibers directly connected the developing retina with the developing lens at this time point. At GW 8, we observed ECM and cells extending from the presumptive ciliary margins to the lens epithelium anteriorly and posteriorly, to become continuous with the pupillary membrane (Figs. 2C–E). These structures likely correspond to microvessels anastomosing with the pupillary membrane. Their ECM stained strongly with fibrillin-1, -2, and -3 antibodies. Although fibrillin-1 strongly stained thick bundles connected to the developing ciliary body and inserting into or attaching to the surface of the lens capsule, fibrillin-2 and -3 staining were more extensive, with additionally stained thinner microfibrils in the ECM between the ciliary margins and the peripheral part of the developing cornea (Figs. 2D,

Investigative Ophthalmology & Visual Science

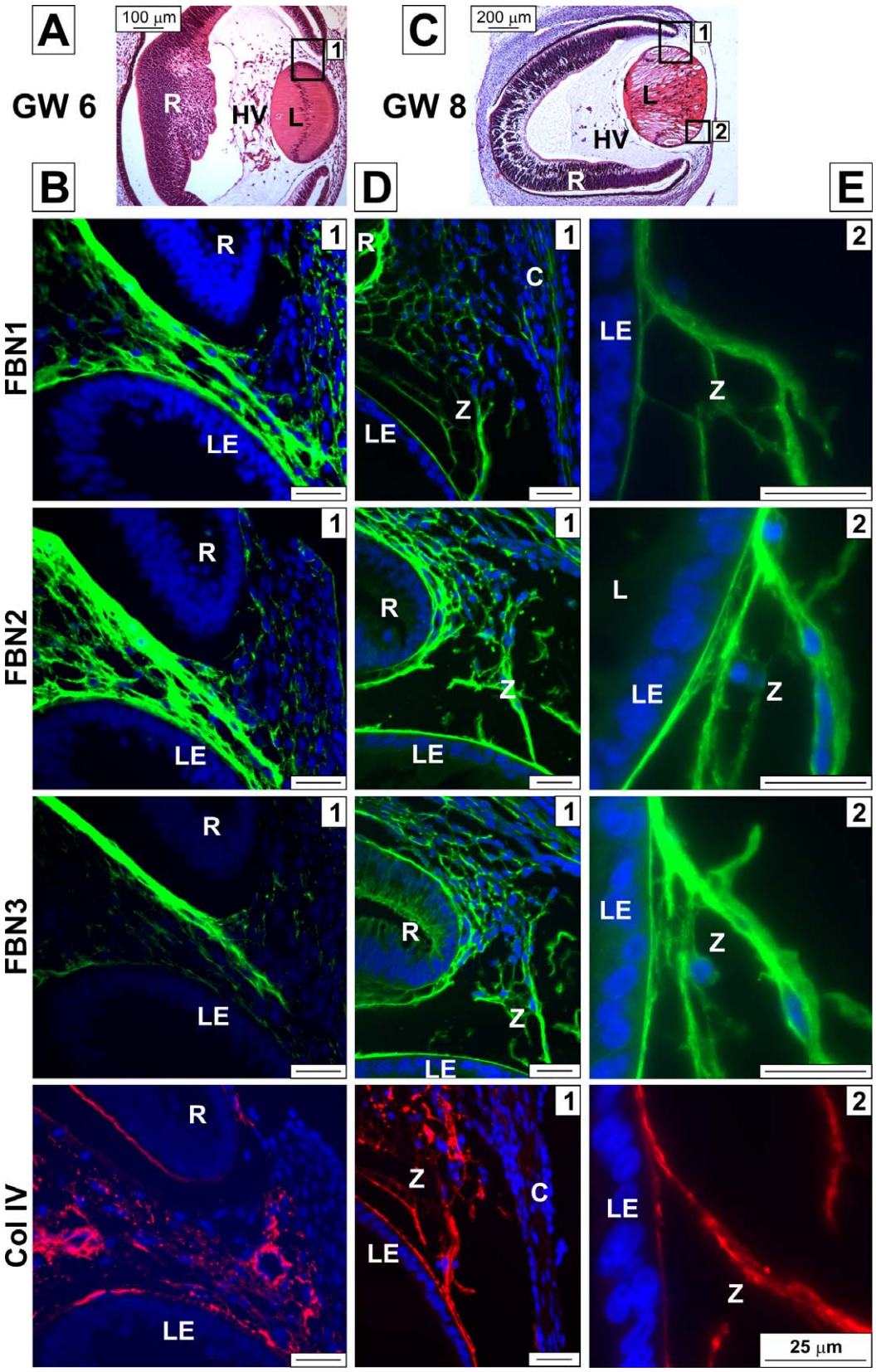

Figure 2. Distribution of fibrillin microfibrils in vascular structures between the prospective ciliary body and the lens in a human eye at GW 8. (**A**) Hematoxylin and eosin–stained guide section shows the boxed areas for which higher magnification images are shown in (**B**). (**B**) Immunostaining for fibrillin-1, -2, and -3 (*green*) and Col IV (*red*) at GW 6. Collagen IV was used as a marker for lens capsule (adjacent to LE) and blood vessels. (**C**) Hematoxylin and eosin–stained guide section shows the boxed areas for which higher magnification images are shown in (**D**, **E**). (**D**) Immunostaining for fibrillin-1, -2, and -3 (*green*) and Col IV (*red*). Collagen IV was used as a marker for lens capsule (adjacent to LE) and blood vessels. (**E**) Higher-magnification images of fibrillin localization with respect to the lens capsule. Note the presence of DAPI-stained nuclei in these

Investigative Ophthalmology & Visual Science

images, whereas the adult zonule is a cell-free structure, and the presence of Col IV in the vascular structure. C, cornea; HV, hyaloid vessels; R, retina; Z, zonule region. *Scale bar*: 25 μm (100 μm/200 μm for H&E panels, as indicated).

2E). This tissue spanning the lens and retina is a vascular structure because it stained with Col IV, a component of basement membranes and a typical marker for primitive vasculature and endothelial cells (Figs. 2D, 2E).[32]

Fibrillin Microfibrils in the Developing Cornea and Lens Epithelium

At GW 8, the central region of the developing cornea is considerably thinner than the periphery. The central region

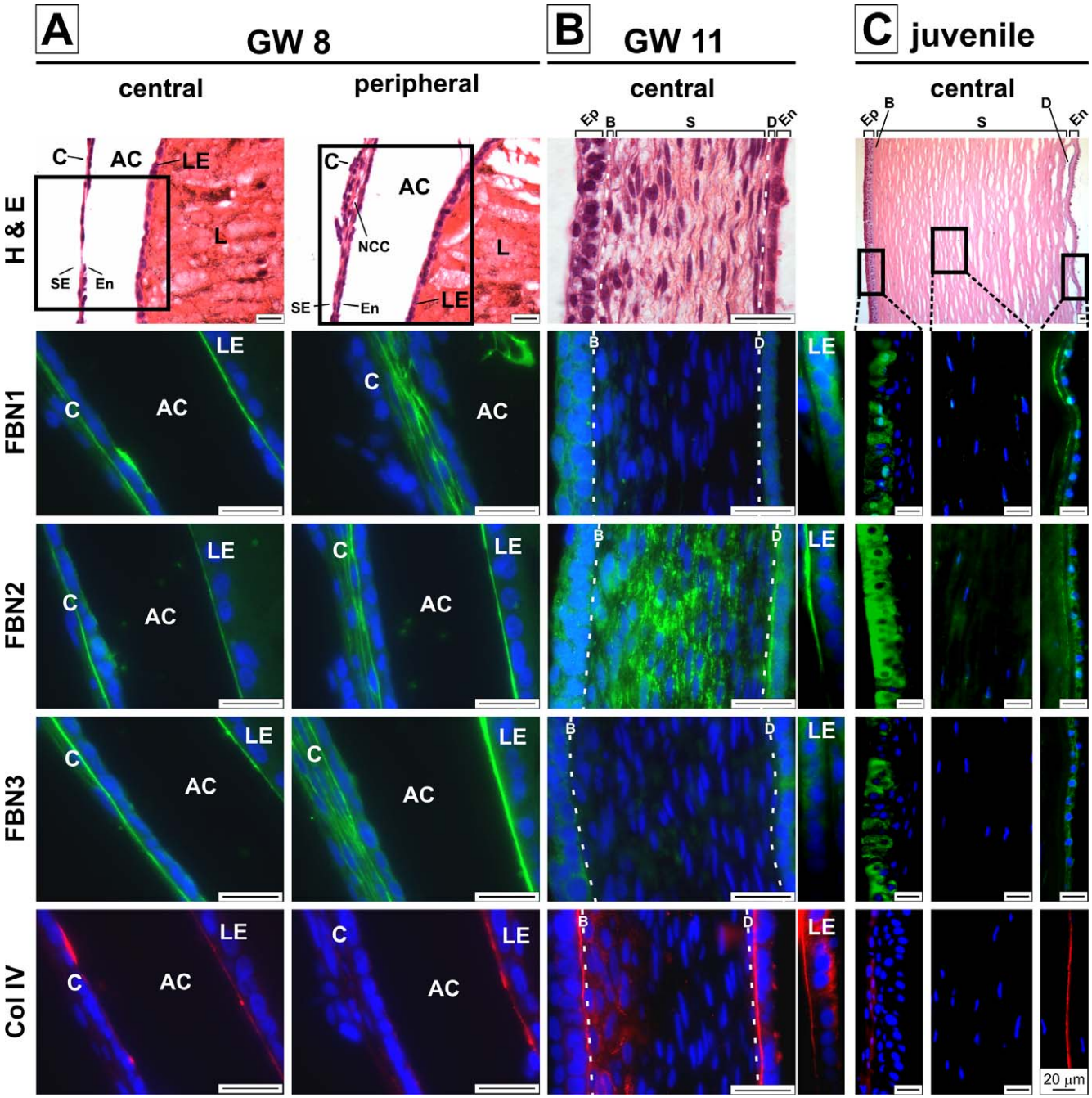

Figure 3. Fibrillins in the developing and juvenile cornea and anterior lens capsule. (**A**) Fibrillin-1, -2, and -3 immunostaining (*green*) of the central (*left-hand column*) and peripheral cornea (*right-hand column*) at GW 8 shows fibrillins in the ECM/prospective basement membranes separating the epithelium from the endothelium and in the lens capsule. (**B**) Fibrillin-1, -2, and -3 immunostaining (*green*) of the central region of the cornea at GW 11. At this stage, the cornea is fully stratified. Only fibrillin-2 could be detected in the stroma. In contrast to the GW 8 cornea, both basement membranes stained for Col IV (*red*). (**C**) Fibrillin localization (*green*) in the central region of the juvenile cornea (3 years of age). Fibrillin-1 and -2 were present in Descemet membrane. The observed epithelial staining is nonspecific. Collagen IV (*red*) was detected in the juvenile (1 year of age) Descemet membrane, but not Bowman's membrane. AC, anterior chamber; B, Bowman's membrane; D, Descemet membrane; En, endothelium; Ep, epithelium; NCC, neural crest cells; S, stroma; SE, surface epithelium. *Scale bars*: 20 μm.

Investigative Ophthalmology & Visual Science

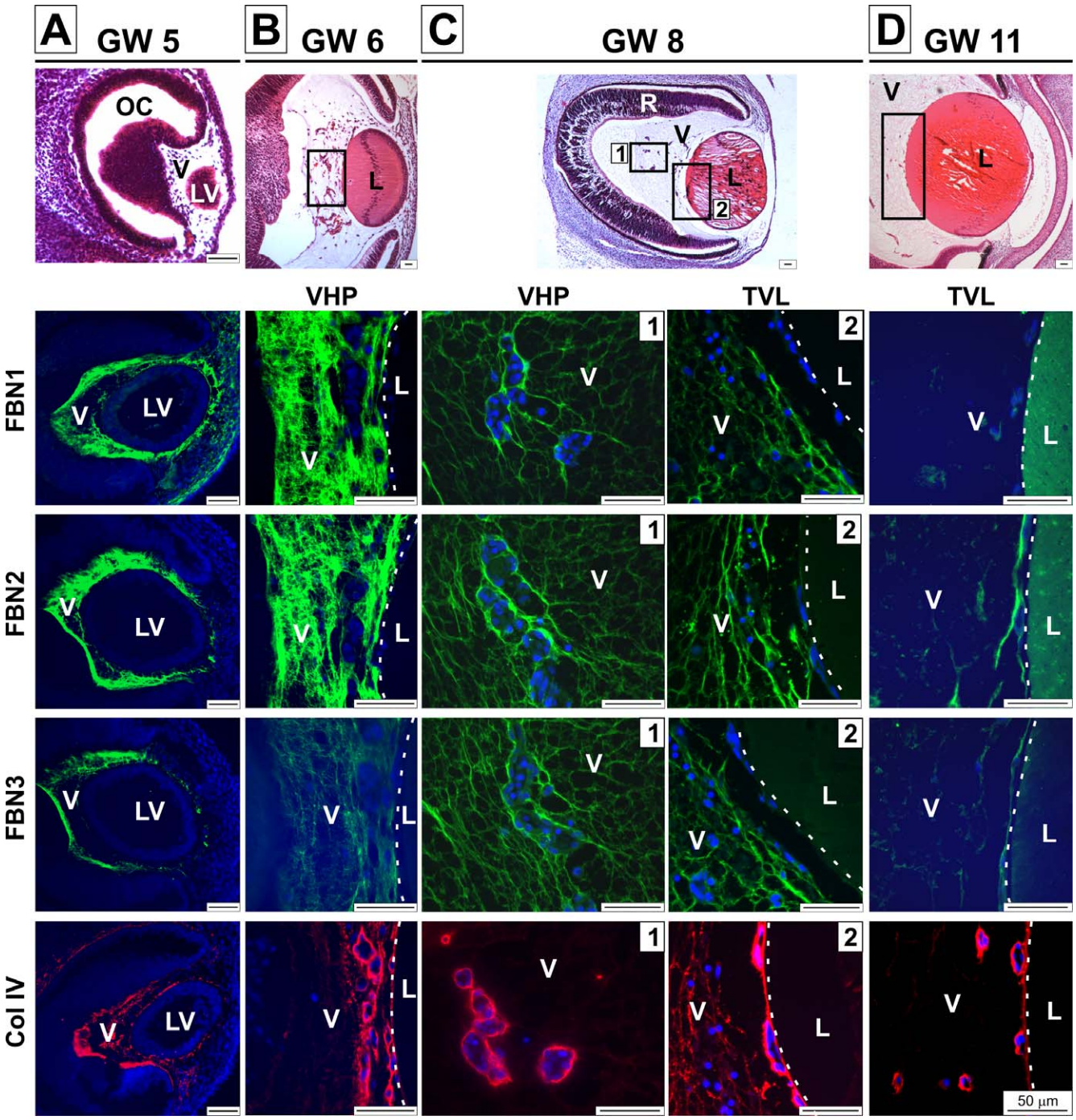

Figure 4. Fibrillin microfibrils in the hyaloid vasculature during development. (**A–D**) Fibrillin-1, -2, and -3 (*green*) and Col IV (*red*) immunostaining of hyaloid vasculature is shown at GW 5 (**A**), GW 6 (**B**), GW 8 (**C**), and GW 11 (**D**). Hematoxylin and eosin–stained guide images (*top*) where the boxed areas indicate the regions shown in the immunostained images. At GW 5 to 6, fibrillin-1, -2, and -3 stained the primary vitreous (**A**, **B**). For GW 8, the VHP (*left*) and the TVL (*right*) are shown (**C**). Fibrillin immunostaining of the TVL is shown at GW 11 (**D**). Collagen IV is used as a marker for blood vessels. EOT, extraocular tissue; LV, lens vesicle; OC, optic cup. *Scale bars*: 50 µm.

consists of two cell layers, corneal epithelium and endothelium, with sparse keratocytes in the prospective corneal stroma (Fig. 3A). This prospective stroma region was positive for fibrillin-1, -2, and -3, but did not stain for Col IV (Fig. 3A). There was focal staining for fibrillin-1 and -2 in the corneal endothelial cells, which also showed patches of Col IV. At its periphery, the developing cornea at GW 8 was multilayered, with a well-established stroma containing abundant keratocytes, and fibrillin-1, -2, and -3 microfibrils, but not Col IV (Fig. 3B). The anterior lens epithelium had a basal lamina positive for fibrillin-1, -2, -3, and Col IV, but the posterior lens capsule was negative for the fibrillin isoforms. At GW 11, the cornea was stratified (from anterior to posterior) into epithelium, Bowman's membrane, stroma, Descemet membrane, and endothelium (Fig. 3B). At this stage, both basement membranes were marked by the presence of Col IV (Fig. 3B). However, although fibrillin-1 and -3 were absent in both basement membranes, fibrillin-2 was a component of Desce-

met membrane, but not Bowman's membrane. The corneal stroma stained strongly for fibrillin-2, but was devoid of fibrillin-1 and -3 microfibrils. The anterior lens capsule and epithelium stained positive for fibrillin-2 and Col IV, but fibrillin-1 and -3 were absent (Fig. 3B, "LE"). In the juvenile eye, fibrillin-1 and -2 were found in Descemet membrane, but were absent in the corneal stroma and Bowman's membrane (Fig. 3C). The observed staining of the corneal epithelium was also seen in negative controls on omission of the primary antibody (data not shown) and is thought to be nonspecific. Collagen IV was present in Descemet membrane, but absent in Bowman's membrane.

Fibrillin Distribution in the Hyaloid Vasculature

At GW 5 to 6, the primary vitreous contained fibrillin-1, -2, and -3 and its vasculature stained strongly for Col IV (Figs. 4A, 4B). At GW 8, we observed strong staining for fibrillin-1, -2, and -3 in the ECM of the vasa hyaloidea propria (VHP), which are branches of the hyaloid artery extending from the retina toward the posterior aspect of the lens during development (Fig. 4C). The vascular identity was supported by the presence of Col IV in the basement membrane (lowest panels) and endomucin staining (data not shown) of endothelial cells. At GW 8, the distribution of the fibrillin isoforms in the ECM of the VHP was more uniform than at GW 5 to 6, and additional delicate fibrous staining was seen in the vitreous with antibodies against each fibrillin isoform compared with GW 6 (Fig. 4C, left-hand column). Interestingly, the tunica vasculosa lentis (TVL) did not contain any fibrillin, but was clearly positive for Col IV (Fig. 4C, right hand column, lowest panel). At GW 11, the staining for fibrillins in the vitreous was much reduced, and only fibrillin-2 could be clearly detected in the ECM of the TVL (Fig. 4D). The hyaloid system had regressed fully in the juvenile eyes.

Fibrillin Distribution in the Ocular Posterior Segment

The mesenchyme surrounding the embryonic optic cup/prospective retina and retinal pigment epithelium forms two layers at GW 6: the choroid and the sclera, respectively. At GW 6, we detected fibrillin-1, -2, and -3 in the choroid and sclera with isoform-specific distribution patterns (Fig. 5A). Fibrillin-1 and -2 were enriched in the ECM of the choroid relative to the sclera, whereas strong staining for fibrillin-3 microfibrils was present in the choroid and sclera. We detected fibrillin-1 microfibrils throughout the sclera, whereas fibrillin-2 staining was confined to scleral tissue adjacent to the choroid. At GW 8, the distribution of the fibrillin isoforms in the choroid was similar to GW 6, except for fibrillin-2, which showed stronger scleral staining than fibrillin-1 or -3 (Fig. 5B). At higher magnification, fibrillin-3 was distributed in punctae and fibers, whereas fibrillin-1 and -2 appeared only as fibrillar structures (Fig. 5B, insets, left-hand column). At GW 11, fibrillin-1 was exclusively found in ECM of the choroid, whereas fibrillin-2 strongly stained the choroid and sclera (Fig. 5C). Fibrillin-3 microfibrils were confined to the choroid and to the scleral ECM adjacent to the choroid. Collagen IV outlined the choroidal/scleral vasculature, consistent with its presence in vascular basement membranes.

At GW 6, the retina consists of the inner neural retina and the outer pigmented retinal epithelium, separated by the intraretinal space (Fig. 5A). At GW 6, the retina stained strongly for fibrillin-3, but was devoid of fibrillin-1 and -2. Fibrillin-3 staining was evident in the ECM of the outer and inner neuroblastic layers, with stronger immunoreactivity in the inner neuroblastic layer. Fibrillin-3 also was enriched in the outer limiting membrane, the nerve fiber layer, and the inner limiting membrane, which stained positive for Col IV (Fig. 5A, bottom). In contrast, fibrillin-3 was absent from the RPE. At GW 8, fibrillin-3 was found in the outer limiting membrane, the nerve fiber layer, and the pericellular matrix of the inner nuclear cells, but was absent from the pericellular matrix of the retinal cells and the inner limiting membrane (Fig. 5B). At GW 11, staining for fibrillin-3 was further reduced in the outer limiting membrane and absent elsewhere in the retina (Fig. 5C). In the juvenile retina, fibrillin-1 and -3 were present in the retinal nerve fiber layer and the outer plexiform layer (Fig. 5D). Fibrillin-3 also was found as fibers or associated with the pericellular matrix of putative bipolar cells, traversing the outer nuclear layer. Fibrillin-2 was absent from the juvenile retina and the observed signal in Figure 5D (central panel) was nonspecific.

MAGP1 Distribution in the Developing Human Eye

MAGP1 was generally codistributed with the fibrillins, without a preferential association with any of the three isoforms. At GW 6, MAGP1 was present between the developing lens and retina, choroid, parts of the retina, and the VHP (Fig. 6A), where it more closely resembled the pattern of fibrillin-3 deposition than the other two isoforms. At GW 8, we found strong staining in the choroid, the VHP, the vitreous, and the vascular structure bridging the ciliary body and the developing lens (Fig. 6B). In the developing central cornea, MAGP1 was present in the prospective stroma and in Descemet membrane. In addition, MAGP1 was found in the lens capsule. At GW 11, MAGP1 staining intensity was generally reduced but immunolocalization clearly showed its presence in ECM of the choroid, the hyaloid vasculature, the nascent zonule, and the VHP (Fig. 6C). It was also localized to the corneal stroma and to lens epithelial cells and lens capsule (Fig. 6C). In the juvenile eye, strong MAGP1 staining was seen in the zonule and at its insertion sites at the ciliary body and the lens (Fig. 6D).

Discussion

We have described here the distribution of all three fibrillin isoforms during human eye development from GW 6 to GW 11 and in juvenile eyes. All three fibrillin isoforms were present in the vascular structure bridging the ciliary body and the lens, the choroid, the VHP, and the vitreous. Isoform-specific distribution of the fibrillins was found in the developing cornea, the lens capsule, and the retina, with a general transition of isoform composition from fibrillin-1, -2, and -3 during development (with fibrillin-2 and -3 prevailing) to preponderance of fibrillin-1 in juvenile tissue. This was consistent with previous reports for ocular and other tissues of rodents and humans.[16,17,21] For example, in mouse eyes at embryonic day 16.5, *Fbn2* expression was high and *Fbn1* expression was low. At postnatal day 1 (P1), *Fbn1* and *Fbn2* expression levels were comparable, but at P30, *Fbn1* expression dominated and it was especially strongly expressed by the nonpigmented ciliary epithelium.[21] In other mouse tissues, such as the lung, the developmental expression of *Fbn1* and *Fbn2* was also temporally regulated.[16] *Fbn2* was transiently expressed exclusively by the bronchial epithelium and diminished after birth, whereas *Fbn1* was expressed in the pulmonary vasculature and mesenchyme.[16] Human fibrillin-3 was most abundant in fetal tissues and was notably found in the brain parenchyma, but was absent from blood vessels.[33]

That the adult human zonule comprises fibrillin-1 microfibrils is well known, but in addition to fibrillin-1, fibrillin-3, and not fibrillin-2, was part of the juvenile zonule.[2,12,19] How the

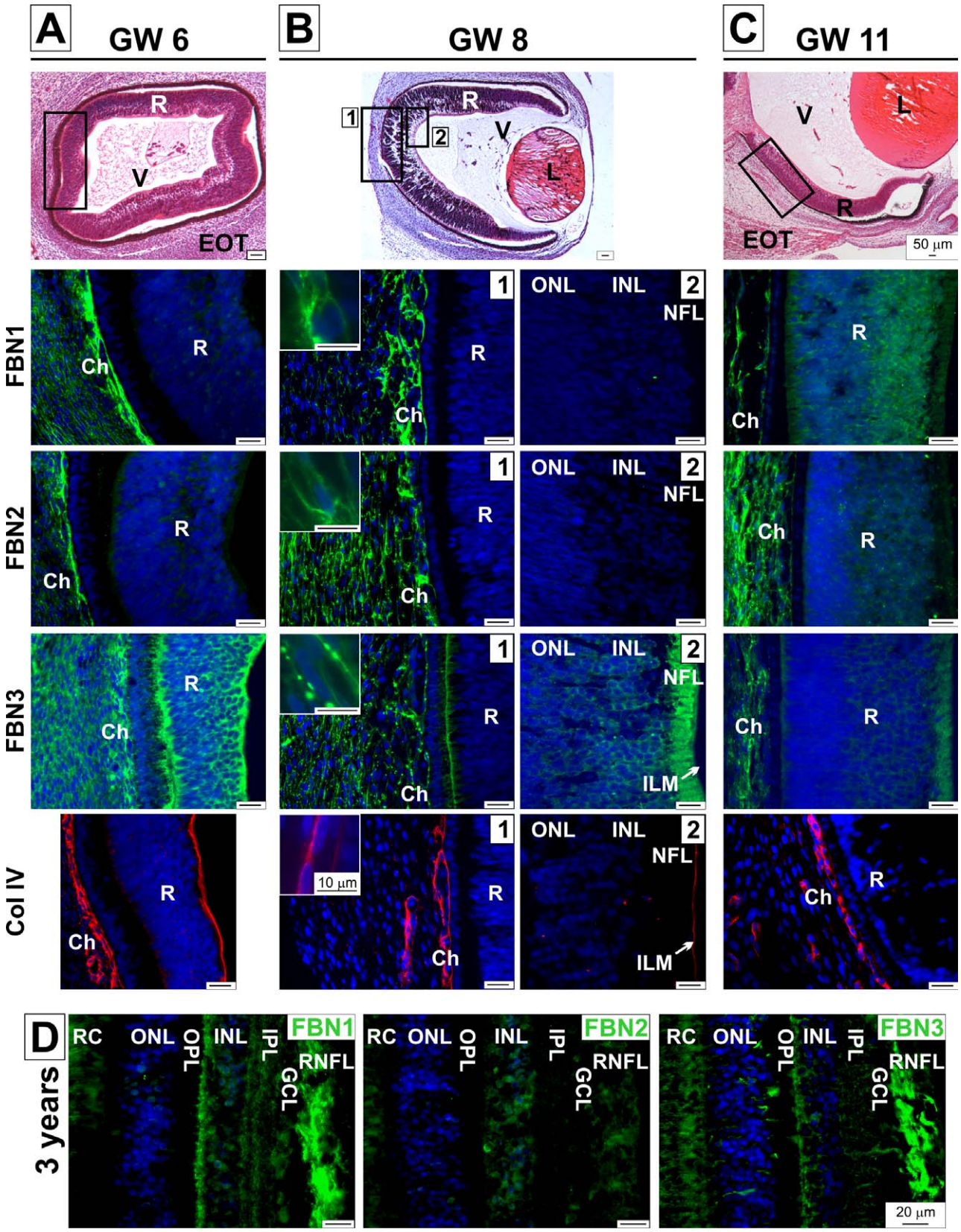

Figure 5. Fibrillin isoforms in the developing retina and the choroid. (**A**–**C**) Hematoxylin and eosin–stained guide images indicate the regions shown by immunostaining. Fibrillin (*green*) and Col IV (*red*) immunostaining is shown at GW 6 (**A**), GW 8 (**B**), and GW 11 (**C**). All fibrillins were present in the choroid, but fibrillin-3 was the only isoform present in the retina. Collagen IV was limited to the choroid and the inner limiting membrane (**A**, **B**). (**D**) Fibrillin immunostaining of juvenile retina showed staining for fibrillin-1 and -3 in the retinal nerve fiber layer and fibrillin-3 was found in the outer plexiform and outer nuclear layer. Ch, choroid; EOT, extraocular tissue; GCL, ganglion cell layer; IPL, inner plexiform layer; INL, inner nuclear layer; RNFL, retinal nerve fiber layer; ONL, outer nuclear layer; OPL, outer plexiform layer; RC, rods and cones. *Scale bars*: 20 μm (50 μm for H&E panel at GW 11).

Investigative Ophthalmology & Visual Science

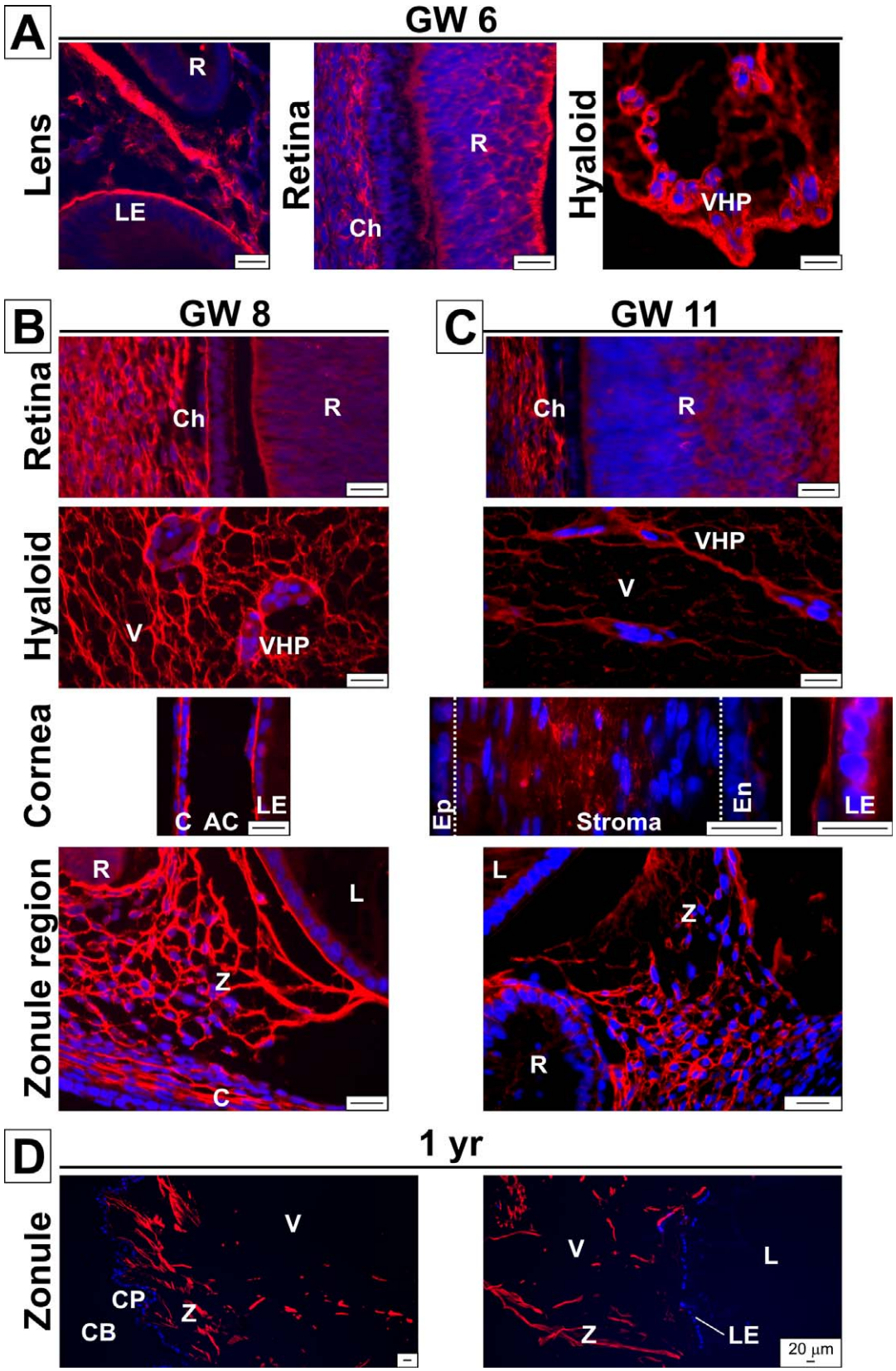

Figure 6. Immunolocalization of MAGP1 in the developing and juvenile eye. (**A–D**) Immunostaining of MAGP1 is shown at GW 5 to 6 (**A**), GW 8 (**B**), GW 11 (**C**), and 1 year of age (**D**). The MAGP1 was generally found in the same location as the fibrillin isoforms shown in preceding figures, including the retina, the hyaloid vasculature, the vascular structure in the zonule region and the lens, and the juvenile zonule. *Scale bars*: 20 μm.

zonule initially forms is not known. Shi et al.[21] proposed that microfibrils, polymerized from fibrillins secreted by the ciliary nonpigmented epithelium, formed the zonule when the ciliary body and the lens were juxtaposed during eye development. We found that the space between the ciliary margin (i.e., the anterior edge of the optic cup), which ultimately forms the ciliary body, and the developing lens, was bridged by a vascular structure that most likely represents an extension of the pupillary membrane. This structure contained all three fibrillin isoforms. We speculate that the first fibers of the future zonule, which is a cell-free structure, may form on, or use this vascular ECM scaffold to bridge the gap between the lens and the ciliary body. The pupillary membrane undergoes regression well before birth and this initial fibrillin-2 and -3–rich perivascular ECM could nucleate the ciliary zonule, which subsequently is predominantly composed of fibrillin-1, secreted by ciliary body and inserted in the lens epithelium.

Interestingly, fibrillin-2 was present in the adult mouse, rat, and hamster zonule and was the sole fibrillin isoform in the zonule of *Fbn1* knockout mice, indicating that it has the potential to compensate for the absence of fibrillin-1 in mice.[13] The adult human and bovine zonules appear to differ in this regard from the mouse, because they do not contain fibrillin-2.[13,19] Importantly, in addition to an integral role for fibrillin microfibrils in the zonule, other ECM proteins are likely to be essential accessory factors for the formation or homeostasis of the zonule. They include ADAMTS10, ADAMTS17, ADAMTSL4, and LTBP2.[23–25,28,29,34] Indeed, ADAMTS10, ADAMTSL4, and LTBP2 have previously been shown to bind to fibrillin-1 and/or modulate its assembly.[22,35–37] Ectopia lentis is also associated with homocystinuria and it was shown previously that homocysteine targeted fibrillin-1 in vitro and interfered with its self-assembly.[38–40] Because the fibrillin isoforms are highly homologous at the protein level, with absolute conservation of the cysteine residues targeted by homocysteine, it can be expected that homocysteine has a comparable detrimental effect on fibrillin-2 and fibrillin-3 as on fibrillin-1, even though this has not been formally tested.[41] Thus, ocular manifestations of homocystinuria, but not of individual fibrillin genes, could affect all three fibrillin isoforms.

In the developing cornea, all fibrillin isoforms were found in the nascent basement membranes at GW 8. At GW 11, only fibrillin-2 was present, and in the juvenile cornea, we found fibrillin-1 and some fibrillin-2 in Descemet membrane. Interestingly, the early corneal basement membranes at GW 8 did not stain for Col IV, whereas the fully formed Bowman's membrane and Descemet membrane were clearly Col IV positive, indicative of a traditional basement membrane. Fibrillins may thus be structural surrogates for typical corneal basement membrane proteins until these are secreted and assembled into a proper basement membrane. Indeed, fibrillin-3 was frequently associated with basement membranes in human tissues other than the eye.[18] The reduction in fibrillin-1 staining in Descemet membrane from infant to adult was described previously.[42] Fibrillin-2 was found in the epithelial basement membrane and was strongly enriched in dystrophic corneas in lattice corneal dystrophy.[20]

The function of fibrillin-3 in the eye remains unclear, mainly because no human mutations causing ocular disease have been reported so far and because the *Fbn3* gene is inactivated in the mouse.[18,33] We found fibrillin-3 in the same tissues as fibrillin-1 or -2, including various ocular basement membranes. Indeed, fibrillin-3 was previously identified in nonocular basement membranes during human development.[18] Interestingly, in the choroid, fibrillin-3 stained as punctae, but elsewhere appeared as fibrillar structures, suggesting different modes of fibrillin-3 assembly, deposition, or interactions in the ECM. Moreover, fibrillin-3 was prominent in the retina, which was mostly devoid of fibrillin-1 and -2. Expression of fibrillin-3 in parts of the nervous system and the brain was also described previously and could indicate a role for fibrillin-3 in neuronal ECM.[18,33]

In summary, we have provided a comprehensive localization of all three fibrillin isoforms during early human eye development. Despite the limitations inherent in sampling only a few developmental and juvenile time points, the findings point out a specific sequence of fibrillin gene expression and distribution in ocular tissues. Thus, a well-orchestrated transition among fibrillin isoforms is likely to be crucial for the formation of the ciliary zonule and other ocular structures. The present study also supports the need for further investigation of the outcome of fibrillin deficiency in ocular structures other than the zonule, which has hitherto been the major focus of most analyses.

Acknowledgments

The authors thank Miriam Linneweh, PhD, and Simone Liebscher, MSc (both University Women's Hospital of the Eberhard-Karls-University Tübingen, Tübingen, Germany), for their assistance with collecting the tissue samples. We are grateful to Robert Mecham, PhD (Washington University, St. Louis, MO, USA), for providing the fibrillin-2 and MAGP1 antibodies.

Supported by the Marfan Foundation Early Investigator Grant (DH), the National Institutes of Health RO1 Grant EY021151 (SSA), the Canadian Institutes of Health Research MOP-106494 (DPR), the Fraunhofer-Gesellschaft Internal Programs Attract 692263 (KS-L), and the Ministry of Science, Research and the Arts of Baden-Württemberg Grants 33-729.55-3/214 and SI-BW 01222-91 (KS-L).

Disclosure: **D. Hubmacher**, None; **D.P. Reinhardt**, None; **T. Plesec**, None; **K. Schenke-Layland**, None; **S.S. Apte**, None

References

1. Hubmacher D, Reinhardt D. Microfibrils and fibrillin. In: Mecham RP, ed. *The Extracellular Matrix: An Overview*. Berlin, Germany: Springer-Verlag; 2011:233–265.
2. Wheatley HM, Traboulsi EI, Flowers BE, et al. Immunohistochemical localization of fibrillin in human ocular tissues. Relevance to the Marfan syndrome. *Arch Ophthalmol*. 1995; 113:103–109.
3. Keene DR, Maddox BK, Kuo HJ, Sakai LY, Glanville RW. Extraction of extendable beaded structures and their identification as fibrillin-containing extracellular matrix microfibrils. *J Histochem Cytochem*. 1991;39:441–449.
4. Nahum Y, Spierer A. Ocular features of Marfan syndrome: diagnosis and management. *Isr Med Assoc J*. 2008;10:179–181.
5. Saricaoglu MS, Sengun A, Karakurt A, Colluoglu Z. Autosomal dominant Weill-Marchesani syndrome and glaucoma management. *Saudi Med J*. 2005;26:1468–1469.
6. Harasymowycz P, Wilson R. Surgical treatment of advanced chronic angle closure glaucoma in Weill-Marchesani syndrome. *J Pediatr Ophthalmol Strabismus*. 2004;41:295–299.
7. Faivre L, Gorlin RJ, Wirtz MK, et al. In frame fibrillin-1 gene deletion in autosomal dominant Weill-Marchesani syndrome. *J Med Genet*. 2003;40:34–36.
8. Takaesu-Miyagi S, Sakai H, Shiroma T, Hayakawa K, Funakoshi Y, Sawaguchi S. Ocular findings of Beals syndrome. *Jpn J Ophthalmol*. 2004;48:470–474.
9. Shi Y, Tu Y, Mecham RP, Bassnett S. Ocular phenotype of Fbn2-null mice. *Invest Ophthalmol Vis Sci*. 2013;54:7163–7173.
10. Ratnapriya R, Zhan X, Fariss RN, et al. Rare and common variants in extracellular matrix gene Fibrillin 2 (FBN2) are associated with macular degeneration. *Hum Mol Genet*. 2014; 23:5827–5837.

11. Traboulsi EI, Whittum-Hudson JA, Mir SH, Maumenee IH. Microfibril abnormalities of the lens capsule in patients with Marfan syndrome and ectopia lentis. *Ophthalmic Genet*. 2000; 21:9–15.
12. Mir S, Wheatley HM, Hussels IE, Whittum-Hudson JA, Traboulsi EI. A comparative histologic study of the fibrillin microfibrillar system in the lens capsule of normal subjects and subjects with Marfan syndrome. *Invest Ophthalmol Vis Sci*. 1998;39:84–93.
13. Beene LC, Wang LW, Hubmacher D, et al. Nonselective assembly of fibrillin 1 and fibrillin 2 in the rodent ocular zonule and in cultured cells: implications for Marfan syndrome. *Invest Ophthalmol Vis Sci*. 2013;54:8337–8344.
14. Lin G, Tiedemann K, Vollbrandt T, et al. Homo- and heterotypic fibrillin-1 and -2 interactions constitute the basis for the assembly of microfibrils. *J Biol Chem*. 2002;277: 50795–50804.
15. Charbonneau NL, Dzamba BJ, Ono RN, et al. Fibrillins can co-assemble in fibrils, but fibrillin fibril composition displays cell-specific differences. *J Biol Chem*. 2003;278:2740–2749.
16. Zhang H, Hu W, Ramirez F. Developmental expression of fibrillin genes suggests heterogeneity of extracellular microfibrils. *J Cell Biol*. 1995;129:1165–1176.
17. Mariencheck MC, Davis EC, Zhang H, et al. Fibrillin-1 and fibrillin-2 show temporal and tissue-specific regulation of expression in developing elastic tissues. *Connect Tissue Res*. 1995;31:87–97.
18. Sabatier L, Miosge N, Hubmacher D, Lin G, Davis EC, Reinhardt DP. Fibrillin-3 expression in human development. *Matrix Biol*. 2011;30:43–52.
19. Cain SA, Morgan A, Sherratt MJ, Ball SG, Shuttleworth CA, Kielty CM. Proteomic analysis of fibrillin-rich microfibrils. *Proteomics*. 2006;6:111–122.
20. Resch MD, Schlotzer-Schrehardt U, Hofmann-Rummelt C, Kruse FE, Seitz B. Alterations of epithelial adhesion molecules and basement membrane components in lattice corneal dystrophy (LCD). *Graefes Arch Clin Exp Ophthalmol*. 2009; 247:1081–1088.
21. Shi Y, Tu Y, De Maria A, Mecham RP, Bassnett S. Development, composition, and structural arrangements of the ciliary zonule of the mouse. *Invest Ophthalmol Vis Sci*. 2013;54: 2504–2515.
22. Inoue T, Ohbayashi T, Fujikawa Y, et al. Latent TGFbeta binding protein-2 is essential for the development of ciliary zonule microfibrils. *Hum Mol Genet*. 2014;23:5672–5682.
23. Morales J, Al-Sharif L, Khalil DS, et al. Homozygous mutations in ADAMTS10 and ADAMTS17 cause lenticular myopia, ectopia lentis, glaucoma, spherophakia, and short stature. *Am J Hum Genet*. 2009;85:558–568.
24. Dagoneau N, Benoist-Lasselin C, Huber C, et al. ADAMTS10 mutations in autosomal recessive Weill-Marchesani syndrome. *Am J Hum Genet*. 2004;75:801–806.
25. Desir J, Sznajer Y, Depasse F, et al. LTBP2 null mutations in an autosomal recessive ocular syndrome with megalocornea, spherophakia, and secondary glaucoma. *Eur J Hum Genet*. 2010;18:761–767.
26. Narooie-Nejad M, Paylakhi SH, Shojaee S, et al. Loss of function mutations in the gene encoding latent transforming growth factor beta binding protein 2, LTBP2, cause primary congenital glaucoma. *Hum Mol Genet*. 2009;18:3969–3977.
27. Christensen AE, Fiskerstrand T, Knappskog PM, Boman H, Rodahl E. A novel ADAMTSL4 mutation in autosomal recessive ectopia lentis et pupillae. *Invest Ophthalmol Vis Sci*. 2010;51: 6369–6373.
28. Ahram D, Sato TS, Kohilan A, et al. A homozygous mutation in ADAMTSL4 causes autosomal-recessive isolated ectopia lentis. *Am J Hum Genet*. 2009;84:274–278.
29. Greene VB, Stoetzel C, Pelletier V, et al. Confirmation of ADAMTSL4 mutations for autosomal recessive isolated bilateral ectopia lentis. *Ophthalmic Genet*. 2010;31:47–51.
30. Weinbaum JS, Broekelmann TJ, Pierce RA, et al. Deficiency in microfibril-associated glycoprotein-1 leads to complex phenotypes in multiple organ systems. *J Biol Chem*. 2008;283: 25533–25543.
31. Tiedemann K, Batge B, Muller PK, Reinhardt DP. Interactions of fibrillin-1 with heparin/heparan sulfate, implications for microfibrillar assembly. *J Biol Chem*. 2001;276:36035–36042.
32. Fruttiger M. Development of the mouse retinal vasculature: angiogenesis versus vasculogenesis. *Invest Ophthalmol Vis Sci*. 2002;43:522–527.
33. Corson GM, Charbonneau NL, Keene DR, Sakai LY. Differential expression of fibrillin-3 adds to microfibril variety in human and avian, but not rodent, connective tissues. *Genomics*. 2004;83:461–472.
34. Hubmacher D, Apte SS. Genetic and functional linkage between ADAMTS superfamily proteins and fibrillin-1: a novel mechanism influencing microfibril assembly and function. *Cell Mol Life Sci*. 2011;68:3137–3148.
35. Gabriel LA, Wang LW, Bader H, et al. ADAMTSL4, a secreted glycoprotein widely distributed in the eye, binds fibrillin-1 microfibrils and accelerates microfibril biogenesis. *Invest Ophthalmol Vis Sci*. 2012;53:461–469.
36. Kutz WE, Wang LW, Bader HL, et al. ADAMTS10 protein interacts with fibrillin-1 and promotes its deposition in extracellular matrix of cultured fibroblasts. *J Biol Chem*. 2011;286:17156–17167.
37. Hirani R, Hanssen E, Gibson MA. LTBP-2 specifically interacts with the amino-terminal region of fibrillin-1 and competes with LTBP-1 for binding to this microfibrillar protein. *Matrix Biol*. 2007;26:213–223.
38. Hubmacher D, Cirulis JT, Miao M, Keeley FW, Reinhardt DP. Functional consequences of homocysteinylation of the elastic fiber proteins fibrillin-1 and tropoelastin. *J Biol Chem*. 2010; 285:1188–1198.
39. Hubmacher D, Tiedemann K, Bartels R, et al. Modification of the structure and function of fibrillin-1 by homocysteine suggests a potential pathogenetic mechanism in homocystinuria. *J Biol Chem*. 2005;280:34946–34955.
40. Sadiq MA, Vanderveen D. Genetics of ectopia lentis. *Semin Ophthalmol*. 2013;28:313–320.
41. Piha-Gossack A, Sossin W, Reinhardt DP. The evolution of extracellular fibrillins and their functional domains. *PLoS One*. 2012;7:e33560.
42. Kabosova A, Azar DT, Bannikov GA, et al. Compositional differences between infant and adult human corneal basement membranes. *Invest Ophthalmol Vis Sci*. 2007;48:4989–4999.

Investigative Ophthalmology & Visual Science